

Aerial Measurement of Sea Surface Temperature in the Infrared¹

PETER M. SAUNDERS²

Woods Hole Oceanographic Institution, Woods Hole, Massachusetts 02543

Measurements made with an airborne radiation thermometer suffer from the imperfect transparency of the atmosphere and the nonblackness of the sea surface. A correction procedure is proposed in which the surface is alternately viewed normally and at an angle near 60° from the normal; the difference between the two measurements is shown to give the required correction. Field tests indicate that an absolute accuracy of $\pm 0.2^\circ\text{C}$ in estimates of surface temperature can be achieved.

Introduction. At the Woods Hole Oceanographic Institution we have been observing the surface temperature of the ocean with an airborne radiation thermometer (radiometer). The instrument employs a thermistor bolometer as detector and a filter transmitting only in the region between 8.25 and 12.35 microns. Its time constant is 1 sec, and its field of view is $4.5^\circ \times 4.5^\circ$. When flown in an aircraft at an altitude of 300 meters, the target spot is 20 meters in diameter. In sharp contrast the depth of ocean perceived is only 20 microns. Because of this characteristic a radiometer determines the temperature at the ocean interface: this value will generally be slightly different from the value of the 'surface' temperature as conventionally measured by an immersion instrument [Saunders, 1967].

In oceanography the usefulness of aerial surveys of 'surface' temperature has to some extent been hindered by the poor accuracy achieved in the observations: uncorrected radiometric measurements have an uncertainty of at least 1°C [Pickett, 1966]. In this paper we shall describe and report the testing of a procedure for improving the absolute accuracy of airborne measurement to $\pm 0.2^\circ\text{C}$ or better. It is our belief that this improvement will be important in studies of the exchange of energy between ocean and atmosphere, in investigations of the evolution of the surface temperature field, especially in the tropics where the

annual range is very small, and quite generally in combined operations involving ships and aircraft where compatibility of the data is required.

As is well known by now, there are two intrinsic problems associated with this technique of measurement; we exclude here the problem of proper instrument calibration which requires that sensitivity checks be made an integral part of the data gathering process. The two problems are (1) the imperfect transparency of the atmosphere between surface and sensor and (2) the nonblackness of the surface itself.

It is proposed that the correction for these two problems be measured *at flight level* by observing the surface first near the normal and then obliquely. The difference in the indicated temperature arises both from the change in air path between sensor and surface and from the change in energy emitted and reflected from the surface. For a nearly transparent atmosphere doubling the air path, by viewing first vertically and then obliquely at 60° from the vertical, doubles the absorption-emission correction; for the ocean this procedure also approximately doubles the correction for nonblackness. Hence the *change* in indicated temperature resulting from the change in angle of viewing is just the correction to be added to the normal value in order to obtain a proper estimate of surface temperature.

The explanation is amplified and the success achieved by the technique is described in the following paragraphs.

Atmospheric absorption and emission. A broad band radiometer measures the specific intensity of radiant energy (or radiance) inte-

¹ Contribution 1876 of the Woods Hole Oceanographic Institution.

² Now (on leave) at the National Center for Atmospheric Research, Boulder, Colorado 80302.

grated over some wavelength region and weighted by the combined spectral properties of its mirror/lens-filter-detector: by calibration the measurement is converted to an equivalent blackbody temperature, which for brevity will be referred to as an *indicated* temperature. The radiant energy determined at flight level differs from that measured near the surface because of attenuation by the intervening atmosphere and because of emission from the atmosphere itself. The indicated temperature at flight level is greater than, equal to, or less than the surface value according to whether the temperature of the atmosphere is greater than, equal to, or less than the surface value. From an altitude of 300 meters differences may amount to $\pm 0.5^\circ\text{C}$ even in the so-called window region.

Smoothed spectral transmission properties of the atmosphere are shown in Figure 1. We have assumed 300 meters of moist atmosphere containing water vapor with a mixing ratio of 15 g/kg. The histogram is calculated from relations given by *Davis and Viezee* [1964]; the crosses computed from *Kondrat'ev et al.* [1966]. The proximity and opaqueness of the 6.3-micron

water vapor band and the 15-micron carbon dioxide band dictates that particular care be exercised in the choice of the filter to minimize the effects of atmospheric absorption. The characteristics of the filter employed in our study are also shown in Figure 1 along with the thermistor bolometer properties [*Wark et al.*, 1962].

Suppose the radiometer views the ocean surface through an atmosphere that is homogeneous in the horizontal but is stratified in the vertical in an arbitrary fashion. If the line of sight is inclined at an angle θ to the vertical the effective mass of absorbing gas measured *down* from flight attitude h to the level z can be written $u(z) \sec \theta$, where $u(z)$ is the effective mass measured down in the vertical direction. In the spectral region under consideration the effective mass of absorbing gas is the mass of water vapor weighted by the ratio of its pressure to a standard pressure, say 1000 mb. The expression for the specific intensity I measured at the radiometer is

$$I(\theta) = B_s \cdot \tau[u(0) \sec \theta] + \int_{z=0}^{z=h} B_a \cdot d\tau[u(z) \sec \theta] \quad (1)$$

where B_s is the specific intensity of the ocean from a near-surface position, B_a is the specific intensity of a blackbody at air temperature (a function of height, z), and $\tau[u]$ is the transmission of the atmosphere, the fraction of the energy transmitted by an effective mass of absorbing gas u . (It is understood that all quantities are integrated over the effective limits of transmission of the filter, namely 8.35–12.2 μ).

Equation 1 can also be written

$$I(\theta) = B_s + \int_{z=0}^{z=h} (B_a - B_s) \cdot d\tau[u(z) \sec \theta]$$

and by making a Taylor expansion of the blackbody function about B_s with good approximation we obtain

$$T_i(\theta) = T_s + \int_{z=0}^{z=h} (T_a - T_s) \cdot d\tau[u(z) \sec \theta] \quad (2)$$

where T_i is the indicated temperature at flight altitude, T_s is the indicated temperature from

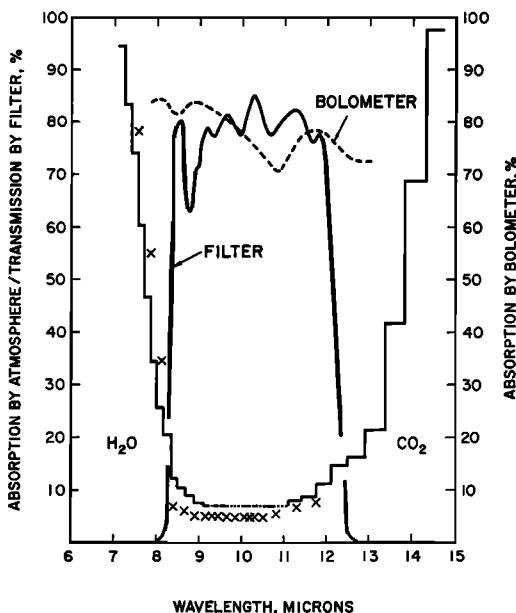


Fig. 1. Spectral properties of the atmosphere and the Woods Hole radiometer. Transmission is shown for a column of 300 meters of air containing water vapor with a mixing ratio 15 g/kg.

a near-surface position, and T_a is the air temperature at height z . We note that, only when $T_a = T_s$, is $T_i = T_s$.

In the case of near transparency the absorption, or $1 - \tau$, is approximately proportional to the effective mass of absorbing gas. Thus

$$1 - \tau = ku \quad (3)$$

where k is the coefficient of absorption. With this approximation

$$\begin{aligned} \delta\tau[u(z) \sec \theta] &= k \sec \theta \delta u(z) \\ &= \sec \theta \delta\tau[u(z)] \end{aligned} \quad (4)$$

and equation 2 can be written

$$T_i(\theta) = T_s + \sec \theta \int_{z=0}^{z=h} (T_a - T_s) \cdot d\tau[u(z)] \quad (5)$$

where

$$T_s = 2T_i(\theta = 0) - T_i(\theta = 60^\circ) \quad (6)$$

which states that the difference between the normal and 60° oblique indicated temperature, when added to the normal value, gives an estimate of the surface temperature corrected for the absorption and emission of the atmosphere.

Because of the nature of the transmission function in the window region it may be shown that the difference between the indicated temperatures at $\theta = 0$ and 60° slightly underestimates the integral in equation 2. Its magnitude is demonstrated by the following example. Suppose a black surface is viewed through 500 meters of isothermal atmosphere containing water vapor with mixing ratio 10 g/kg that is 5°C warmer than the underlying surface. From the work of *Kondrat'ev et al.* [1966] we put $\tau = \exp -0.1u$ and find that the indicated temperature will be 0.45° and 0.85°C warmer than the surface temperature for normal and 60° oblique viewing respectively. The analysis of *Davis and Viezee* [1964] suggests instead that $\tau = \exp -(0.1 u)^{0.88}$ and the indicated temperatures are then 0.6° and 1.1°C warmer than the surface for $\theta = 0$ and 60° . The normal-oblique difference, in these calculations, underestimates the absorption-emission correc-

tion for normal viewing by 0.05° and 0.1°C , errors acceptable in our measurements.

Radiant energy reflected from the sea surface. That the sea is slightly reflecting is illustrated in Figure 2. The passage of the aircraft from regions with a clear 'cold' sky to regions where there is a dense overcast of 'hot' low cloud gives rise to an increase in the indicated temperature. It is inferred that there is little change in the true surface temperature since the observed changes are close to the calculated change for the measured reflectivity of the surface (Table 1).

We have made an experimental determination of the reflectivity of a plane water surface over a range of angles of incidence from 15° to 80° . Hot and cold sources of infrared radiation are viewed by our radiometer both directly and via reflection in a clean plane water surface. The ratio of the differences in energy from the two sources first received via reflection and then directly measures the reflectivity of the surface. Our values agree extremely closely with the values computed³ from the generalized Fresnel relations employing the complex refractive index tabulations of *Cen-teno* [1941]. (See Table 2.) At near normal incidence the measured reflectivity is $1.12 \pm .03\%$, but we should emphasize that this value (along with the others in Table 2) depends on the particular spectral properties of our instrument.

The surface of the ocean is, of course, rarely plane, and the optical properties of a rough surface will generally differ from the optical properties of a plane surface. Accordingly, we have investigated the reflectivity of the ocean, making use of both observational and theoretical approaches. The theory is an extension of the work of *Cox and Munk* [1954] and is based on a description of the statistics of the surface slopes. This work will be reported in detail in a future paper; here we shall merely quote the relevant conclusions. Provided that measurements are averaged over a statistically adequate sample of waves on the sea surface, a condition automatically met in the normal operation of our airborne radiometer, the re-

³ Computations performed and kindly made available to the author by R. M. Schotland of New York University.

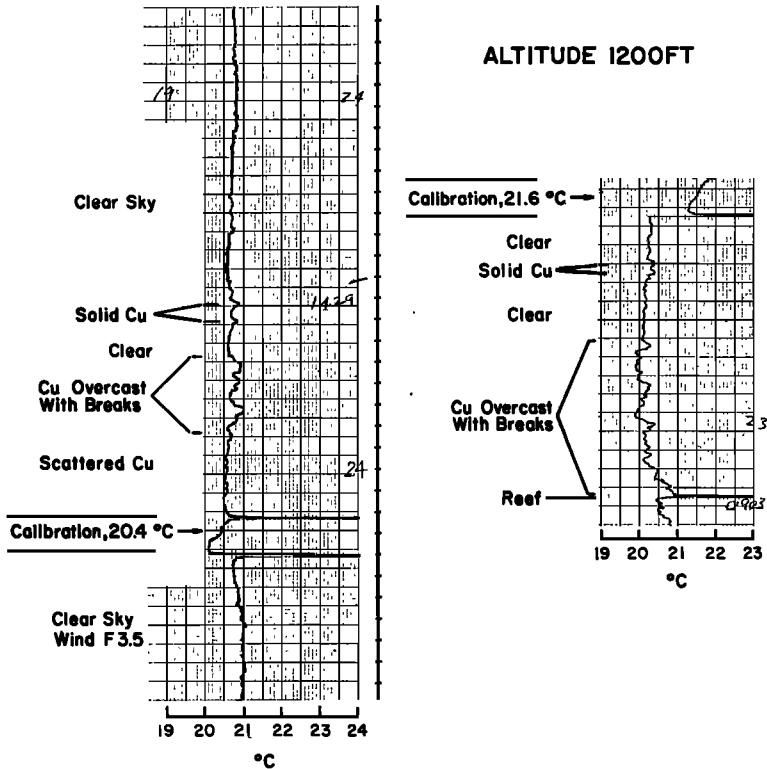


Fig. 2. The influence of low clouds overhead on the temperature indicated by an airborne radiometer.

flectivity of the ocean when viewed almost normally is insignificantly different from the reflectivity of a plane surface. Indeed, with an error that is at most 10%, we can assume that the reflectivity values of Table 2 are ap-

propriate to the ocean for a range of angles of incidence from 0 to 55°. On the other hand, near the horizon the optical characteristics of the ocean are found to be quite different from those of a plane surface.

TABLE 1. Correction (To Be Added) to the Indicated Temperature of the Sea Surface Arising from Nonblackness, under Clear Skies

Date	Correction for Reflection at Near Normal Incidence, °C	Air Temperature, °C	Angle at Which Correction Is Doubled, deg
Jan. 14, 1966	0.75	2.0	53
Mar. 2, 1966	0.7	6.1	53
Oct. 25, 1965	0.7	10.0	56
May 3, 1966	0.65	8.3	53
Oct. 18, 1965	0.65	12.7	53.5
Oct. 20, 1965	0.55	17.5	56
July 18, 1966	0.55	21.5	56
June 14, 1966	0.5	18.4	57
Aug. 18, 1966	0.45	21.8	57.5
Aug. 17, 1966	0.4	22	57

The specific intensity I measured from a near surface location is given by the expression

$$I = B - r(B - I^\dagger) \tag{7}$$

where B is the blackbody intensity at the surface temperature, I^\dagger is the sky intensity viewed in the appropriate direction, and r is the reflectivity for the appropriate angle of incidence. (The role played by the sun in reflection is discussed in an appendix.)

The second term of (7) measures the correction for nonblackness, and, since the sky is generally colder than the surface, $I^\dagger < B$, the indicated temperature is less than the true temperature of the surface, $I < B$. Because $B - I^\dagger$ is very large, it is not permissible to linearize the Planck function here as was done,

TABLE 2. Reflectivity of a Plane Water Surface in the 8.35 to 12.2- μ Region

Angle of Incidence, deg	Measurements, %	Reflectivity,* %
0 (normal)	...	1.15
15	1.12 \pm .03	...
30	1.18 \pm .03	1.21
40	1.38 \pm .03	1.43
50	2.11 \pm .04	2.12
55	3.00 \pm .07	2.92
60	4.33 \pm .10	4.29
70	10.9 \pm .3	10.93
75	17.8 \pm .55	18.4
80	31.0 \pm 1.3	31.8
90 (grazing)	...	100

* Computed from electromagnetic theory and tabulations of *Centeno* [1941].

in equation 2. From a pier we have made measurements of the sea and sky emission with a radiometer with spectral characteristics identical with those of our airborne instrument but with larger dynamic range and a field of view of only $0.5^\circ \times 0.5^\circ$. Combining these measurements with the reflectivity determinations of Table 2, we have deduced from equation 7 the nonblackness corrections shown in Table 1. Under clear skies values range from 0.4° to 0.75°C (with our instrument), depending primarily on season, and only under an overcast of low cloud, when $B - I^\dagger$ becomes small, is the correction negligible.

Because reflectivity increases with angle of incidence (Table 2) and because the sky is generally cold, the indicated temperature of the surface of the ocean decreases with increasing obliqueness of viewing. Typical measurements are shown in Figure 3, where the magnitude of the difference of the indicated from true surface temperature has been obtained at one point on each curve, at an angle near 30° , from equation 7 as outlined above. By this procedure we can estimate the angle of viewing required to double the nonblackness correction for near normal viewing. Values for this angle, shown in Table 1, range seasonally from 53° to 57.5° , and the variation results from differing distributions of sky intensity I^\dagger with zenith angle. The clear sky emission, which depends on the distribution of temperature and humidity in the atmosphere, is more nearly isotropic in winter, when the atmosphere has low water content, than it is in

summer. The presence of stratiform cloud does not change these angles appreciably; it does of course reduce the magnitude of the nonblackness correction.

The variation in angle is an unfortunate drawback to the proposed normal-oblique method of investigation and leads one to consider alternative procedures. By measuring humidity and air temperature at flight level and by relying on the coherence of these properties in the lowest 300 meters of atmosphere over the ocean we suppose that the absorption-emission correction of equation 2 might be estimated with the required accuracy. (We take note of the data reduction program accompanying this procedure.) Similarly, by measuring sky intensity at flight level the nonblackness correction could be determined from equation 7. The in-flight determination of sky intensity would probably mean the permanent installation of a second radiometer, which is costly; in addition, the dynamic range of many instruments in use (our airborne radiometer included) would not permit them to measure the low-energy levels of sky emission without nontrivial modification.

In the face of these problems the normal-

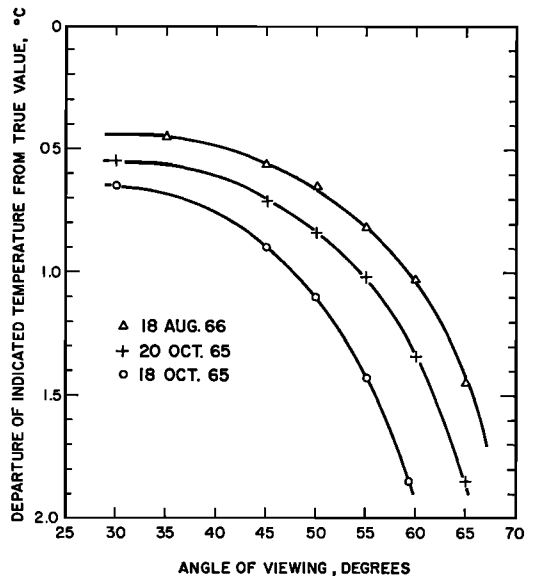


Fig. 3. Near surface measurements of the difference between indicated and true surface temperature of the ocean as a function of angle of viewing under clear skies.

TABLE 3. Comparison of Aerial and Bucket Measurements

Aerial Measurements		Shipboard Measurements							
Conditions	Time	Indicated Temperature at		Corrected Surface Temperature, °C	Bucket Temperature, °C	Air Temperature, °C	Dew Point, °C	Time	Ship
		Flight Level, °C	Temperature, °C						
Altitude, 365 meters. Sky clear. Air temperature, 17.3 °C. Dew point, 11.2 °C. Normal-oblique difference: 60°, 0.55 °C; 55°,	1152	18.3 ± .1	18.85 ± .1	18.85 ± .1	19.1	20.0	15.6	1152	R. V. Crawford
	1156	18.2 ± .1	18.75 ± .1	18.75 ± .1	19.1			1156	42°27'N, 69°33'W Wind, f4
	1207:30	18.3 ± .1	18.85 ± .1	18.85 ± .1					
	1232	18.15 ± .1	18.7 ± .1	18.7 ± .1	19.0	20.3	15.6	1235	
	1240	18.1 ± .2	18.65 ± .2	18.65 ± .2	18.8			1250	
Altitude, 365 meters. Multilayer altocumulus clouds. Air temperature, 19.6 °C. Dew point, 10.2 °C. Normal-oblique difference: 60°, 0.5 °C; 55°, 0.4 °C.	1432	19.2 ± .1	19.7 ± .1	19.7 ± .1	19.8	19.9		1431	R. V. Gosnold
	1435	19.25 ± .1	19.75 ± .1	19.75 ± .1	19.9	19.8		1434	40°03'N, 69°01'W
	1438	19.15 ± .2	19.65 ± .2	19.65 ± .2	20.0	19.8		1437	Wind, f2.5
Altitude, 370 meters. Solid altocumulus overcast. Air temperature, 17.5 °C. Dew point, 11.0 °C. Normal-oblique difference: 60°, 0.45 °C; 55°, 0.3 °C.	1043	17.55 ± .1	18.0 ± .15	18.0 ± .15	18.3	19.0		1043	R. V. Gosnold
	1048	18.1	18.55	18.55	18.9	19.0		1047	Wind f3
	1052	18.15	18.6	18.6	18.8	18.9		1055	
	1100	17.5	17.95	17.95	17.7	18.8		1102	
	1106	17.15	17.6	17.6	17.8	18.7		1107	
	1112	17.55	18.0	18.0	18.1	18.6		1112	
	1147	17.85	18.3	18.3	18.3	18.9		1147	
	1152	17.9	18.35	18.35	18.5	18.9		1152	
	1156	17.75	18.2	18.2	18.5	18.9		1155	
	1200	17.9	18.35	18.35	17.9	18.9		1200	
	1258	19.6 ± .1	20.3 ± .2	20.3 ± .2	20.75	22.6	14.7	1258	R. V. Crawford
	1303	19.45	20.15	20.15	20.5	22.0	15.3	1300	Wind, f2
	1308	19.4	20.1	20.1	20.4	22.5	15.0	1308	
1310	19.45	20.15	20.15	20.4	22.2	14.4	1311		
1315	19.5	20.2	20.2	20.6	21.9	15.0	1315		
1319	19.6	20.3	20.3	20.6	21.9	14.5	1320		
1325	19.9	20.6	20.6	20.9	21.2	14.4	1325		
1329	19.9	20.6	20.6	21.0	20.8	14.7	1329		
1334	20.0	20.7	20.7	20.9	20.9	14.7	1334		

TABLE 3. (Continued)

Aerial Measurements			Shipboard Measurements					
Conditions	Time	Indicated Temperature at Flight Level, °C	Corrected Surface Temperature, °C	Bucket Temperature, °C	Air Temperature, °C	Dew Point, °C	Time	Ship
Altitude, 335 meters. Broken cirrus. Air temperature, 20.8 °C. Dew point, 14.5 °C. Normal-oblique correction: 60°, 0.7°C; 0.55°, 0.55°C.			<i>August 26, 1966</i>					
		22.45 ± .1	23.15 ± .15	23.4	24.5	18.6	1109	R. V. <i>Crawford</i>
		22.45	23.15	23.3	24.9	18.3	1112	39°44'N, 69°58'W
		22.45	23.15	23.3	24.2	18.1	1115	Wind, 13.5
		22.4	23.1	23.3	24.7	18.1	1121	
		23.35	23.05	23.3	24.4	17.8	1124	
		22.4	23.1	23.3	24.6	17.9	1144	

oblique method is seen to possess an attractive simplicity, despite the need of experience in judging the appropriate angle for oblique viewing. We propose that the difference between near normal and oblique both 55° and 60° from the vertical be measured. In warm humid situations (water temperature 20°–25°C) the correction deduced from the 60° angle should be employed and in cold dry situations (water temperature 0–5°C) the correction deduced from the 55° angle should be employed; interpolation procedures can be used for intermediate situations. These angles represent a compromise between the requirements for the best estimates of both the nonblackness and absorption-emission corrections.

Conclusions. Because the optical head of the Woods Hole instrument is large, it is mounted rigidly in our aircraft. In level flight we choose to view the surface at 30° from the normal on the starboard side, so that left-hand turns with bank angles of 25° and 30° lead to oblique viewing of the surface at 55° and 60°, respectively. Clearly this aspect of our procedure is not essential to the technique, and tilting a small radiometer is probably more convenient. We make no attempt to view exactly the same area of the surface both normally and obliquely but rely on horizontal uniformity over distances of about 500 meters. Generally the correction is best estimated by choosing regions in which the surface temperature is quiet; only in rare circumstances of extreme surface variability are there difficulties in making the determination. Because of the low level of turbulence generally encountered over the ocean and because of the inertia of the aircraft (its wingspan exceeds 30 meters), we find that the auto-pilot generally maintains a roll angle within $\pm 1^\circ$. The uncertainty of angle leads to errors in determining the correction of between 0.05° and 0.1°C (under clear skies).

On several occasions we have flown over surface vessels, and measurements made with the radiometer have been compared with conventional dip-bucket observations. The radiometric corrections were obtained by the normal-oblique viewing method (the results are shown in Table 3). During these flights calibration checks were made between every pass, employing an anodized metal plate of known black-

ness, whose temperature was adjusted to correspond closely to that of the surface being measured. The plate was either heated above or cooled below ambient by means of a thermoelectric device.

As in previous flights over surface vessels, the corrected interface temperatures are found to be lower than the bulk water values [Saunders and Wilkins, 1966]. For the five rendezvous reported in Table 1 the mean differences were 0.25°, 0.2°, 0.2°, 0.35°, and 0.2°C, differences comparable to those reported earlier by us and also by Hasse [1963], who used quite different methods of measurement.

We believe this limited body of data demonstrates the achievement of the goal described in the introduction to this paper, namely a significant increase in the accuracy achieved in the remote measurement of ocean surface temperature. Because of the difference between the interface and 'surface' temperatures it is not possible from our measurements alone to demonstrate the final precision attained: the results and discussion above should make plausible a claim of $\pm 0.2^\circ\text{C}$.

APPENDIX

In this appendix the extent to which reflected solar energy influences radiometric measurements of the surface temperature of the ocean will be discussed. It will be demonstrated that in the 8- to 12-micron region radiometry has a day and night capability.

The image of the sun seen by reflection in a rough sea is spread over a large glittering area: the glitter area exists throughout the entire electromagnetic spectrum including, of course, the visible and infrared. If the undistorted image of the zenith sun were viewed in a dead calm sea and if it entirely filled the field of view of a radiometer sensitive in the 8- to 12-micron region, it is readily shown that the indicated temperature would be approximately 100°C above the surface value. The effect in a rough sea can be estimated in the following way. On a rough surface with root mean square slope σ the angular radius of the glitter pattern is seen to be approximately 2σ , and hence the solid angle it subtends is $\pi(2\sigma)^2$. Now the solid angle subtended by the mirror image of the sun is $\pi\epsilon^2$, where ϵ is the angular radius of the sun's disk. If the total radiant energy reflected

from the surface is independent of roughness, the ratio of the intensity in the glitter pattern to the intensity in the mirror image is in the inverse ratio of the solid angles that they subtend, namely $(\epsilon/2\sigma)^2$. For $\sigma = 0.1$ this ratio has a value 5×10^{-4} , and hence temperature anomalies can be expected at the 0.05°C level.

Accurate calculations have been made of the effect of sun glitter on radiometry by employing an isotropic Gaussian function for the slopes of the surface and the relations given in Cox and Munk [1954]. These values are presented in Figures 4 and 5 and substantiate the order of magnitude argument used above. We can summarize the results by asserting that a radiometer directed nearly normal to the surface will not be affected by sun glitter at the 0.1°C level except in very calm seas. When viewed obliquely the glitter pattern can give rise to hot spots of up to 1°C in amplitude, but they have limited angular size, less than 5° in azimuth, and again appear in very calm seas. When the sea is of average roughness, $\sigma = 0.2$,

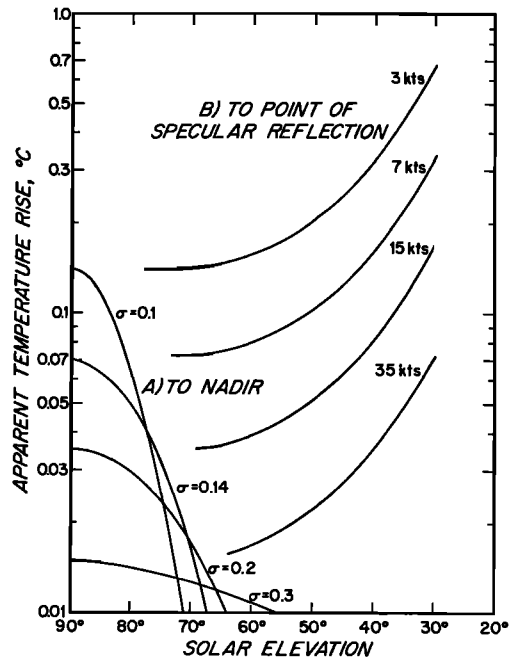


Fig. 4. The apparent temperature increase arising from the reflection of direct solar radiation from the sea surface as a function of roughness. σ is the root mean square slope. (a) Radiometer directed normally, (b) radiometer directed to point of specular reflection.

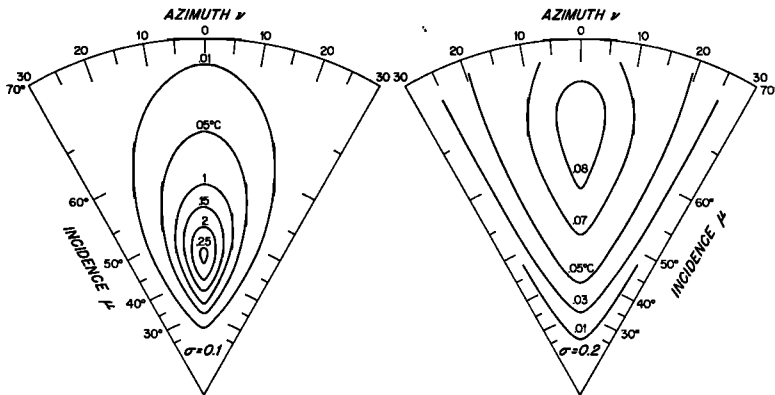


Fig. 5. 'Hot spot' resulting from the reflection of solar radiation from sea surface. Solar elevation 45° . (Left) root mean square slope $\sigma = 0.1$, wind approximately 3 knots; (right) $\sigma = 0.2$, wind 15 knots.

there is a large glitter area with a temperature anomaly unimportant in our work.

Because of the increasing ratio of solar to terrestrial emission, all the shorter wavelength windows of the atmosphere give rise to much larger amplitude glitter effects: for the Nimbus HRIR window, 3.6–4.0 microns, even in large glitter patterns anomalies of 20°C arise.

Acknowledgments. The author is greatly indebted to C. H. Wilkins for technical assistance, to the captain and crew of the C54 aircraft for their willing cooperation, and to Dr. G. L. Clarke and Dr. J. V. A. Trumbull for their participation in the ship-aircraft experiments.

The research was made possible under grant Co.241 from the Office of Naval Research.

REFERENCES

- Centeno, M. V., The refractive index of liquid water in the near-infrared spectrum, *J. Opt. Soc. Am.*, *31*, 244–247, 1941.
- Cox, C., and W. Munk, Measurements of the roughness of the sea surface from photographs of the sun's glitter, *J. Opt. Soc. Am.*, *44*, 838–850, 1954.
- Davis, P. A., and W. Viezee, A method for computing infrared transmission through atmospheric water vapor and carbon dioxide, *J. Geophys. Res.*, *69*, 3785–3794, 1964.
- Hasse, L., On the cooling of the sea surface by evaporation and heat exchange, *Tellus*, *15*(4), 363–366, 1963.
- Kondrat'ev, K. Ya., Kh. Yu. Niilsk, and R. Yu. Noorma, The spectral distribution of the infrared radiation in the free atmosphere, *Izv. Atmospheric Oceanic Phys., English Transl.*, *2*, 70–79, 1966.
- Pickett, R. L., Environmental corrections for an airborne radiation thermometer, *Proc. 4th Symp. Remote Sensing of Environment, Ann Arbor, Michigan*, 259–262, 1966.
- Saunders, P. M., The temperature at the ocean-air interface, *J. Atmospheric Sci.*, *24*, 269–273, 1967.
- Saunders, P. M., and C. H. Wilkins, Precise airborne radiation thermometry, *Proc. 4th Symp. Remote Sensing of Environment, Ann Arbor, Michigan*, 815–826, 1966.
- Wark, D. Q., G. Yamamoto, and J. Lienesch, Infrared flux and surface temperature determinations from Tiros radiometer measurements, *Meteorol. Satellite Lab. Rept. 10*, U. S. Weather Bureau, 1962.

(Received January 16, 1967.)